

# Electron identification and hadron discrimination using Cherenkov radiation in air and SiPMs

**A. Alici,<sup>a,b</sup> F. Carnesecchi,<sup>b,1</sup> B.R. Achari,<sup>a,b</sup> N. Agrawal,<sup>a,b</sup> P. Antonioli,<sup>b</sup> S. Arcelli,<sup>a,b</sup> F. Bellini,<sup>a,b</sup> S. Bufalino,<sup>c,d</sup> D. Cavazza,<sup>b</sup> L. Cifarelli,<sup>a,b</sup> F. Cindolo,<sup>b</sup> G. Clai,<sup>e,b</sup> M. Colocci,<sup>a,b</sup> F. Ercolelli,<sup>a,b</sup> G. Fabbri,<sup>a,b</sup> D. Falchieri,<sup>b</sup> C. Ferrero,<sup>d</sup> A. Ficarella,<sup>f</sup> U. Follo,<sup>c,d</sup> M. Garbini,<sup>g,b</sup> S. Geminiani,<sup>a,b</sup> G. Gioachin,<sup>h</sup> A. Gola,<sup>f</sup> D. Hatzifotiadou,<sup>b</sup> A. Khuntia,<sup>b</sup> A. Margotti,<sup>b</sup> G. Malfattore,<sup>a,b</sup> R. Nania,<sup>b</sup> F. Noferini,<sup>b</sup> L. Parellada-Monreal,<sup>f</sup> M. Penna,<sup>f</sup> O. Pinazza,<sup>b</sup> R. Preghenella,<sup>b</sup> M. Razza,<sup>a,b</sup> R. Ricci,<sup>b</sup> L. Rignanese,<sup>b</sup> A. Rivetti,<sup>c,d</sup> G. Romanenko,<sup>a,b</sup> N. Rubini,<sup>a,b</sup> E. Rovati,<sup>a,b</sup> B. Sabiu,<sup>a,b</sup> E. Scapparone,<sup>b</sup> G. Sciolli,<sup>a,b</sup> S. Strazzi,<sup>a,b</sup> S. Tomassini,<sup>a,b</sup> and A. Zichichi<sup>a,b</sup>**

<sup>a</sup>*Dipartimento di Fisica e Astronomia "A. Righi", University of Bologna, viale Carlo Berti Pichat 6/2, Bologna, 40127, Italy*

<sup>b</sup>*INFN, Sezione di Bologna, viale Carlo Berti Pichat 6/2, Bologna, 40127, Italy*

<sup>c</sup>*Dipartimento di elettronica e telecomunicazioni, Politecnico di Torino, Corso Duca degli Abruzzi, 24, Torino, 10129, Italy*

<sup>d</sup>*INFN, Sezione di Torino, Via Pietro Giuria 1, Torino, 10125, Italy*

<sup>e</sup>*ENEA, Sede di Bologna, Via dei Mille 21, Bologna, 40121, Italy*

<sup>f</sup>*Fondazione Bruno Kessler, Via Sommarive 18, Povo, 38123, Italy*

<sup>g</sup>*Museo Storico della Fisica e Centro Studi Enrico Fermi, Via Panisperna 89 A, Roma, 10129, Italy*

<sup>h</sup>*Dipartimento di Scienza Applicata e Tecnologia (DISAT), Politecnico di Torino, Corso Duca degli Abruzzi 24, Torino, 10129, Italy*

*E-mail:* [francesca.carnesecchi@bo.infn.it](mailto:francesca.carnesecchi@bo.infn.it)

**ABSTRACT:** This paper presents a method to identify electrons using the Cherenkov light emitted when a charged particle travels in air and photons are detected with a Silicon PhotoMultiplier (SiPM). The analysis is based on a photon-counting approach using SPAD cells and uses data collected during a test beam at CERN PS. The results are well described by a simple Monte Carlo simulation, which further demonstrates that a very good electron identification and a strong pion/hadron rejection could be obtained over a wide momentum range.

**KEYWORDS:** Particle identification methods, Cherenkov detectors, Photon detectors for UV, visible and IR photons (solid-state)

---

<sup>1</sup>Corresponding author.

---

## Contents

<b>1</b>	<b>Introduction</b>	<b>1</b>
<b>2</b>	<b>Experimental setup and analysis method</b>	<b>2</b>
2.1	Detectors	2
2.2	Beam test setup	2
2.3	Analysis method	2
<b>3</b>	<b>Results</b>	<b>4</b>
<b>4</b>	<b>Comparison with simulation</b>	<b>4</b>
<b>5</b>	<b>A simple optimization of the key parameters</b>	<b>6</b>
<b>6</b>	<b>Conclusions</b>	<b>9</b>

---

## 1 Introduction

In [1–4] it was quantitatively shown that the Cherenkov radiation produced at the passage of a charged particle through the standard, factory-supplied protection layer of the SiPM itself can produce very high number of firing cells (SPADs with area tens of microns square). Considering a refractive index of 1.56 and a thickness of few hundreds micron for the Silicone material of the protection layer, the Cherenkov angle reaches  $\approx$ 50 degrees, covering a quite large area of few mm<sup>2</sup>. In these conditions it is possible to directly detect charged particles and reach very good efficiency and time resolution around 20 ps [3, 4]. These results opened the possibility to use just a single SiPM as an optimal detector for Time Of Flight (TOF) measurements.

The results reported in the above papers also indicate a very reduced number of firing SPADs when no protection layer is present. For such sensors, events with more than one SPAD are mainly due to cross-talk processes [3, 4].

However, considering particles traversing air before impinging on the SiPM, the Cherenkov effect should still occur for high beta values. This implies that for electrons, even at low energies, there could be an excess of photons emitted at very small angles. Consequently, this would lead to an increase in the number of firing SPADs around the particle’s impact point on the SiPM. Particles like pions, kaons or protons would instead not produce such an effect till they reach a momentum higher than 5.7, 20 or 38 GeV/c respectively. As a consequence, unambiguous identification of electrons would be possible up to  $\sim$ 5-6 GeV/c by simply identifying events with SiPMs without any protection layer and a number of SPADs in excess of the cross-talk. This cell-counting procedure is based on the amplitude of the SiPM signal and its characteristic structure, in which each peak corresponds to a fired SPAD.

To test the above possibility, in this paper data collected at T10 test beam at CERN with momenta from 1.5 to 10  $\text{GeV}/c$  are used. The apparatus is the same described in [3]. At lower momenta the fraction of electrons/positrons in the beam increases thus allowing to compare the SiPM (without protection) signal with the one observed for pions and protons. In Section 2 the experimental set-up and the analysis methods are described. The results are reported in Section 3 and will be compared with a simple simulation in Section 4. In Section 5 a possible optimization of the parameters involved in such study (length of air traversed, different traversed gas, different SiPM technology) is discussed.

## 2 Experimental setup and analysis method

### 2.1 Detectors

For the present study NUV-HD-LFv2 SiPMs produced by Fondazione Bruno Kessler (FBK) were used [5–7]. These detectors have an active area of  $3.20 \times 3.12 \text{ mm}^2$  filled with 6200 SPADs with square pixel pitch of  $40 \mu\text{m}$ , 83% fill factor and breakdown voltage  $V_{bd} = 32.2 \pm 0.1 \text{ V}$  [8, 9]. In this paper only sensors without any protection layer are studied.

### 2.2 Beam test setup

The SiPMs were tested at the CERN PS T10 particle beam in the momentum range 1.5–10  $\text{GeV}/c$ . The beam composition, evaluated via simulation and data, is reported in [10]: while at high momenta the beam is mainly made of protons and  $\pi^+$ , at lower energies the fraction of positrons increases and becomes dominant. In the following, we will neglect the charge, which is unimportant for our purposes, and use generically the terms pions and electrons.

The apparatus was made of a telescope with four sensors: two SiPMs under test and two LGAD detectors ( $1 \times 1 \text{ mm}^2$  area and  $35 \mu\text{m}$  or  $25 \mu\text{m}$  thick sensors) [11]. The latter were used as timing reference and were placed at the beginning and at the end of the telescope to define, through their coincidence, a trigger for the beam particles. The four sensors were placed at a distance of about 7 cm one from the other. Each sensor was mounted on a remotely controlled movable frame capable of positioning with  $10 \mu\text{m}$  precision in both directions perpendicular to the beam axis, ensuring accurate alignment with the beam line. For the SiPM without protection layer the copper Faraday cage, usually used to shield the front-end electronics, had a hole (with area around  $35 \text{ mm}^2$ ) to allow the photons produced in the preceding 7 cm of air to reach the sensor. The SiPM signals were coupled to a customized front-end with X-LEE amplifiers<sup>1</sup> with a total gain factor of about 40 dB. The set-up was inserted into a light-tight box and is the same as described in details in [3]. All sensors were operated at ambient temperature. Waveforms from all four sensors were recorded via a Lecroy Wave-Runner 9404M-MS digital oscilloscope.

### 2.3 Analysis method

The analyzed data were collected with a beam momentum of 1.5  $\text{GeV}/c$  (a second sample at 10  $\text{GeV}/c$  was also collected to check the simulation). The reason for this choice is twofold: first, it enhances the electron component in the beam, which is composed of approximately 60% electrons,

---

<sup>1</sup><https://www.minicircuits.com/pdfs/LEE-39+.pdf>

28% pions, and 12% protons [10]. Second, it enables the separation of electrons and pions from protons by exploiting the time of flight between the signals from the two LGAD detectors placed at the ends of the telescope, as visible in Fig. 1 left (more details in [3]). In the figure a q-Gaussian fit [12] was applied on both distributions.

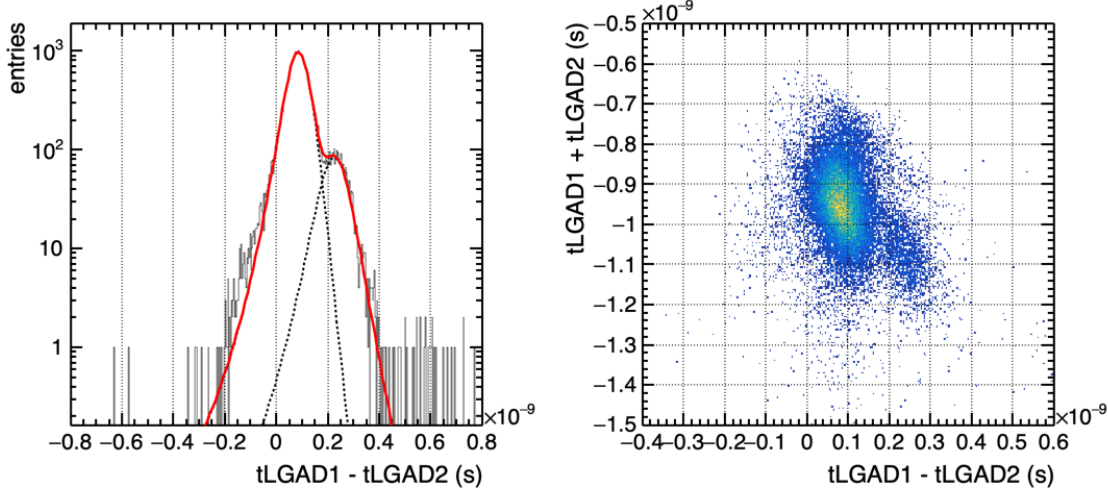


**Figure 1.** Left panel: time of flight of the beam particles computed as the time difference between the two LGADs in the telescope at  $1.5 \text{ GeV}/c$ . The fits are performed with two q-Gaussian, the left one relative to the proton content. Right panel: LGAD time sum versus time difference distribution.

At this beam momentum, electrons are the only particles that produce Cherenkov radiation in the air gap between sensors in the telescope. Electrons and pions cannot be distinguished using the LGADs' time information; however, their charge spectra can still be determined. The proton charge spectrum is used as a proxy for pions normalized to the expected pion fraction [10], since neither pions nor protons are able to generate Cherenkov radiation in air.

The protons sample has been selected with rectangular cuts on the LGAD time sum versus time difference distribution (Fig. 1 right) as  $0.2 < t_{LGAD1} - t_{LGAD2} < 0.4 \text{ ns}$  and  $-1.2 < t_{LGAD1} + t_{LGAD2} < -0.85 \text{ ns}$  while for electrons and pions the cuts are  $0 < t_{LGAD1} - t_{LGAD2} < 0.16 \text{ ns}$  and  $-1.2 < t_{LGAD1} + t_{LGAD2} < -0.7 \text{ ns}$ . With these cuts the fraction of protons remaining in the electron/pion sample is below 1%, while the electron/pion contamination in the proton sample is  $\approx 4\text{-}5\%$ .

The SiPM signals used in the analysis are those within a window of  $\pm 2 \text{ ns}$  from the ( $t_0$ ) trigger given by the coincidence of the two LGAD sensors. The baseline of the acquired waveforms is subject to fluctuations due to the electromagnetic noise present in the experimental area, the dark count rate of the SiPM and high particle rate inducing overlapping signals. To address this, a time window was defined in the interval preceding the signal window, from  $-10 \text{ ns}$  to  $-2 \text{ ns}$  relative to the trigger time  $t_0$ , within which the mean and RMS of the signal amplitude were calculated. To remove events affected by spurious signals, noise, or after-pulses from previous events, all events with a baseline RMS greater than  $0.75 \text{ mV}$  were rejected (14% of the total number of events).

### 3 Results

The data were collected at  $p = 1.5$  GeV/c supplying the SiPM with an overvoltage (OV) of 2 V. This setting, although not optimal to distinguish between electron and hadron signals, was chosen to prevent signal saturation on the vertical scale of the oscilloscope and to ensure a good separation of signals corresponding to different numbers of fired SPADs per event.

The measured amplitudes for the proton sample is reported in Fig. 2 top-left: as expected, it is peaked at one SPAD ( $\sim 31$  mV), with the entries at 0 mV (0 SPAD) compatible with the value of the fill factor of the sensor and with peaks at 2 and 3 SPADs due to crosstalk. The amplitude distribution for pions is expected to be identical to that of protons. The electron distribution is then obtained by taking the amplitude distribution of events identified as electron/pion candidates and subtracting the proton distribution, normalized to the expected pion fraction of 32%[10]. The pion/electron spectrum is reported in Fig. 2 top-right with the estimated fraction of pions and electrons. The electron spectrum, after the pion subtraction, is instead reported in Fig. 2 bottom.

Despite the low overvoltage, the two distributions are clearly distinguishable. Since a single SPAD signal is measured to have an amplitude of 31 mV, selecting tracks with  $\geq$  two SPADs (threshold set at  $\sim 50$  mV) one gets a hadron rejection of  $\approx 85\%$  with an electron selection efficiency of  $\approx 57\%$ .

### 4 Comparison with simulation

The results reported in the previous section rely mainly on the purity of the selected proton sample and on an accurate knowledge of the actual composition of the particle beam. To estimate the impact of these experimental uncertainties the results were cross-checked against the predictions of a toy Monte Carlo (MC) simulation to assess their robustness. The simulation works as follows: two hits are randomly generated on the two LGADs and the track is then propagated to the SiPM. The number of Cherenkov photons created in the air volume upstream the sensor has been calculated based on the Frank-Tamm formula [13]. The detection efficiency for the charged particle was assumed equal to the fill factor according to the manufacturer's specifications, as well as the crosstalk and the PDE as a function of the photon wavelength and SiPM overvoltage. The amplitude distribution is obtained by multiplying the number of fired cells by the average amplitude of 1 SPAD signal assumed as 31 mV according to the acquired data. A gaussian spread of 3.3 mV was applied driven by data observation. Given the binary nature of the SPAD response, multiple photons hitting the same pixel are counted as one. A still-not-fully-satisfactory modeling of the noise is applied to the simulated data based on the measured RMS of the baseline which, however, does not appear to have a significant effect on data reproducibility.

A qualitative comparison between the measured spectra and MC predictions is shown in Fig. 3. In the left pad, the measured amplitude spectrum for protons with a momentum of 1.5 GeV/c is compared with simulations. Here and in the following, the two histograms under comparison are normalized to the same number of entries. The measured spectrum shows a small peak at 3 SPADs which is not predicted by the toy MC. This discrepancy ( $\sim 3\%$  of events with more than 2 SPADs) mainly arise from a small electron contamination in the proton sample selected by LGAD timing information,  $\sim 2 - 3\%$ ; the remaining part may originate from events in which crosstalk affects more

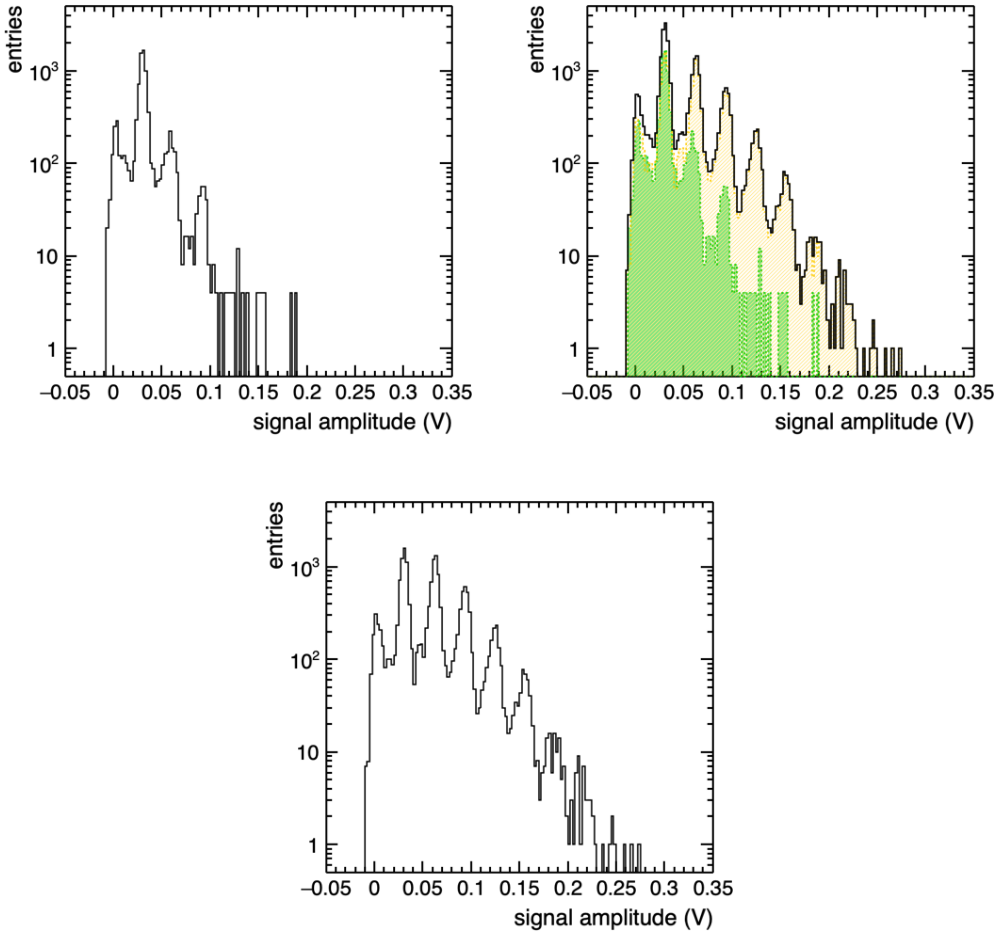


**Figure 2.** Real data at 1.5 GeV/c. Top left: signal amplitude for the proton sample selected. Top right: amplitude for pions and electrons with the estimated fraction of pions (green dotted area) and electrons (orange dashed area). Bottom: the estimated signal amplitude for electrons once the pion contribution (distribution expected to be identical to the protons one) is subtracted.

NUV-HD-LFv2, 3.20×3.12 mm<sup>2</sup>, OV = 2V, thickness<sub>air</sub> = 7 cm.

than one pixel, which is not included in the MC, or from particle near the border of two SPADs. In the same figure the right panel shows a comparison between measured amplitude spectra and simulations at a beam momentum of 10 GeV/c. At this momentum, the beam consists mainly of pions (30%) and protons (70%)[10], with pions producing Cherenkov radiation in air, while protons remain below threshold. In this case, the agreement between the two distributions is qualitatively good and the problems noticed in the previous plot are less evident due to the higher number of SPADs firing. Finally, Fig. 4 compares the measured and simulated amplitude spectra for electrons at 1.5 GeV/c : here too, the comparison shows good agreement.

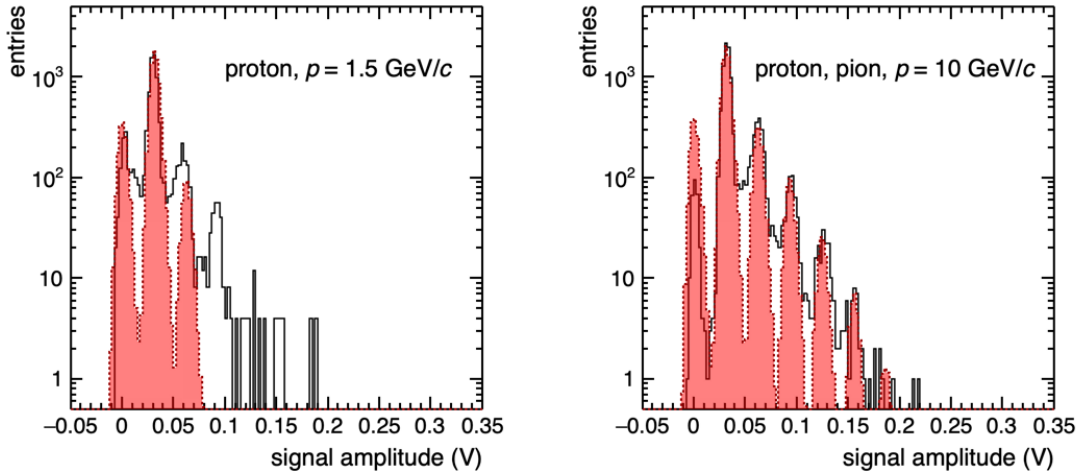


**Figure 3.** Amplitude distribution of data (full line) and MC simulation (red area) for protons at  $1.5 \text{ GeV}/c$  (left) and protons/pions at  $10 \text{ GeV}/c$  (right). NUV-HD-LFv2,  $3.20 \times 3.12 \text{ mm}^2$ , OV = 2V, thickness<sub>air</sub> = 7 cm.

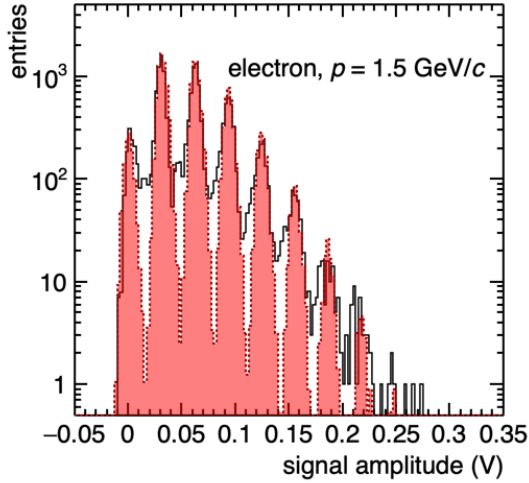


**Figure 4.** Amplitude distribution of data (full line) and MC simulation (red area) for electrons at  $1.5 \text{ GeV}/c$ . NUV-HD-LFv2,  $3.20 \times 3.12 \text{ mm}^2$ , OV = 2V, thickness<sub>air</sub> = 7 cm.

## 5 A simple optimization of the key parameters

Before using the toy MC to obtain an approximate estimate of the potential performance of such a system, a number of parameters were optimized. It was observed that the SiPM coverage has a significant impact, with larger covered areas able to collect more photons produced by the incident charged particle. No significant changes in performance were observed reducing the cell size, within the range tested. A comparison was therefore made between SiPMs with active areas of  $3.20 \times 3.12 \text{ mm}^2$ , as the one used in the test beam data, and a hypothetical  $6 \times 6 \text{ mm}^2$ , both featuring

square SPADs with a pitch of 40  $\mu\text{m}$ . To determine the optimal thickness of the air layer in front of the sensor, the simulation considers particles impinging the SiPM in the center. The over-voltage was set to 6 V.

The optimization was carried out using the plot shown in Fig. 5, where the electron efficiency was calculated considering particles with  $1.5 \text{ GeV}/c$  of momentum and by selecting only events in which three or more SPADs were fired. As can be seen, while below 4 cm the curves relative to the two different size SiPM overlap, at higher distances the larger-area SiPM exhibits a significantly higher efficiency and this is due to the larger surface area, which allows more Cherenkov photons to be collected. The figure also indicates that for the  $6 \times 6 \text{ mm}^2$  sensor beyond 15 cm of air no appreciable variations in the number of collected photons are observed due to the limited size of the simulated sensor. In the following simulations, the response of the larger SiPM will be considered using a distance of 15 cm of traversed air. Notice that the goal of this paper is to investigate the method to identify particles via the SiPM response and there is no attempt to optimize the detector configuration as it should be done for specific applications.

Since electron identification is performed by considering signals with an amplitude higher than the cross-talk value, it is clear that this value represents a fundamental parameter. Recently, the FBK NUV-HD SiPM technology has been upgraded with metal-filled deep trench isolation (NUV-HD-MT [14]) between the SiPM cells, which enables an almost complete suppression of internal optical cross-talk. In the simulation, therefore, in order to select the optimal configuration for the proposed detector, the cross-talk values measured by FBK for this new technology were used. The PDE also impacts performance, as it parameterizes the probability of detecting the produced Cherenkov photons. Assuming the validity of the simulation also at overvoltages higher than 2 V, a value of 6 V was chosen to profit of the higher PDE. The cross-talk and PDE values corresponding to OV = 6 V were taken from [14].

Figure 6 shows electron efficiency and pion rejection as a function of the incoming particle's momentum from the toy MC simulations, for two different selection cuts (number of fired SPADs  $\geq 2$  and  $\geq 3$ ). In addition to the case with air ( $n = 1.00029$ ) as radiator,  $\text{CO}_2$  ( $n = 1.00045$ ) was also considered, as it is an inert, non-flammable gas with low environmental impact and low cost; moreover, its use could be advantageous in configurations where the system requires cooling below the dew point. For both radiator gases, a pion rejection close to 100 % with an electron efficiency larger than  $\sim 85 \text{ \%}$  looks achievable (larger than  $\sim 90 \text{ \%}$  with  $\text{CO}_2$ ). The choice of radiator gas leads to a shift in the results as a function of momentum. When air is used, a separation between electrons and charged hadrons can be achieved from about  $50 \text{ MeV}/c$  up to  $\sim 6 \text{ GeV}/c$ , whereas  $\text{CO}_2$  allows an operation down to momentum values below  $30 \text{ MeV}/c$  and up to  $4 \text{ GeV}/c$ .

Given the threshold nature of the Cherenkov effect and the binary response of the SPADs, it is possible to define momentum regions where, although the identification of individual particles is not always feasible, an appropriate selection based on the number of fired pixels allows discrimination among different particle species.

The results, obtained for a  $6 \times 6 \text{ mm}^2$  SiPM with 15 cm of air as radiator and an overvoltage of 6 V, show that the number of fired SPADs can serve as a practical and tunable handle for particle discrimination. In particular, accordingly to Table 1, low-momentum electrons and very high-momentum protons can each be effectively separated, while at the same time it is possible to set high rejection criteria for the different species in other momentum ranges.

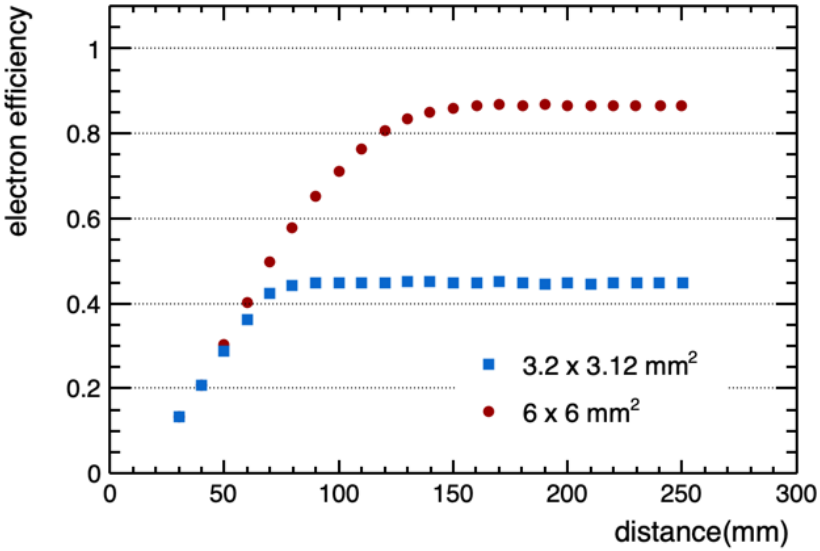


**Figure 5.** Electron detection efficiency versus the distance in air traversed by the particle. Electrons of  $1.5 \text{ GeV}/c$  and two different SiPMs surfaces are considered. The Toy- MonteCarlo parameters used are: NUV-HD-MT, OV = 6 V, Thr = 3 SPAD.

**Table 1.** Particle selection in different momentum ranges based on the number of fired SPADs for a  $6 \times 6 \text{ mm}^2$  SiPM and 15 cm of air gap.

$p$ (GeV/c)	selection	$e$ efficiency	$\pi$ rejection	$K$ rejection	$p$ rejection
0.05 – 6	$\text{nSPAD} \geq 3$	0.86	0.95	1	1
$p$ (GeV/c)	selection	$e$ rejection	$\pi$ rejection	$K$ efficiency	$p$ efficiency
6 – 21	$\text{nSPAD} < 3$	0.86	0.84	0.96	1
$p$ (GeV/c)	selection	$e$ rejection	$\pi$ rejection	$K$ rejection	$p$ efficiency
21 – 40	$\text{nSPAD} < 3$	0.86	0.86	0.78	0.96

Starting from the excellent timing capability of SiPM with a protection layer reported in [3], the approach discussed in the present paper suggests that configurations with two consecutive SiPMs, one without and one with protection layer, with an air gap in front of the first one, could be used to simultaneously support electron identification and TOF measurements, potentially covering PID and particle rejection in different momentum ranges.

Such configurations would be of great interest in particle physics experiments, including space applications. However, the limited radiation hardness of the SiPMs especially in the harshest radiation environments as HL-LHC, remains an important aspect to be addressed.

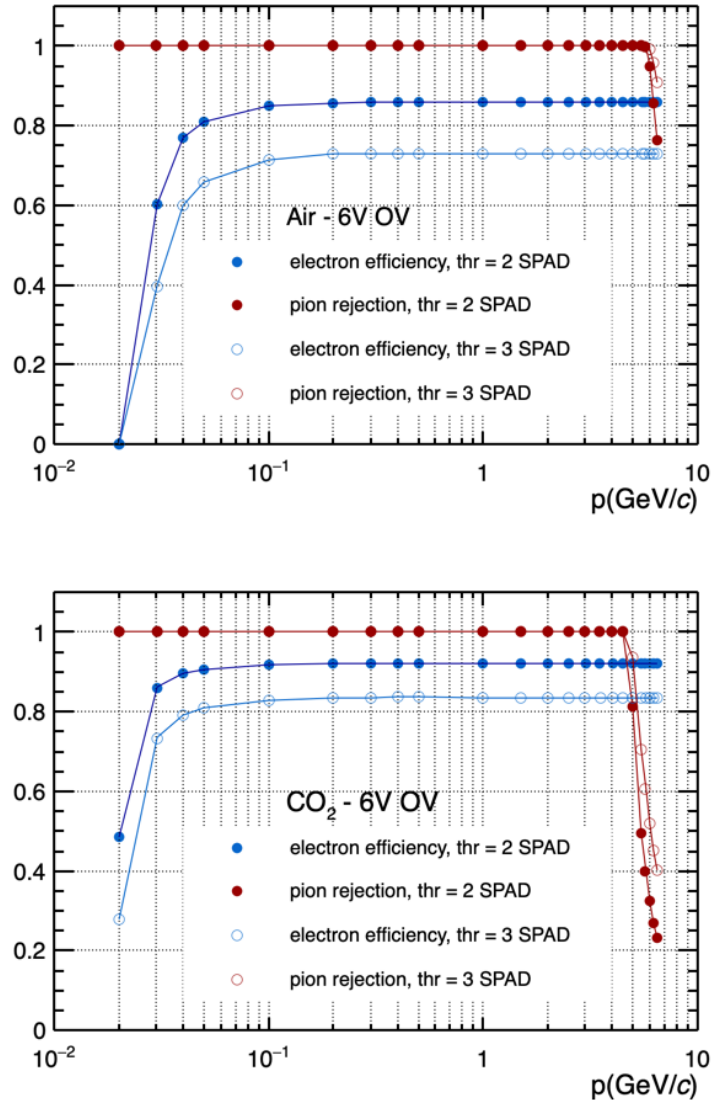


**Figure 6.** MC simulation of electron efficiency and pion rejection versus the momentum for two different selection cuts (number of fired SPADs  $\geq 2$  and  $\geq 3$ ). The Toy- MonteCarlo parameters used are: NUV-HD-MT,  $6 \times 6 \text{ mm}^2$ , OV = 6V, thickness<sub>air/CO<sub>2</sub></sub> = 15 cm.

## 6 Conclusions

In this paper we have studied the possibility to use SiPMs, without coupling to scintillator and without any protection layer, to identify electrons simply using the excess of firing cells (SPADs) produced by the Cherenkov photons emitted by the electron when traversing an air region just before the sensor. Test beam data with 1.5 GeV/c particles results indicate a very good electron identification and a corresponding very high pion rejection. Data are well reproduced with a simple Monte Carlo simulation which includes the photons produced by the Cherenkov effect in air and the SiPM detection parameters.

The MC has also been used for a first simple optimization of the detector parameters indicating, for the case of 15 cm traversed air and a SiPM of  $6 \times 6 \text{ mm}^2$  area, the possibility of an electron identification above 85% in the region 0.05 to 6 GeV/c with a corresponding pion rejection above 96%. This identification technique allows also to use the SPADs counting method to discriminate, in specific very high momentum regions, different particle species (K and p).

Together with the already published results on timing performances of SiPMs with a protection layer [3, 4], the present results underline that the Cherenkov light produced in the simplest radiators in front of the SiPM, i.e. the factory-supplied silicone protective resin or the air, allow these photo-sensors to become themselves optimal detectors for charged particle identification both via time of flight or via photon counting measurements.

## Declarations

This project has received funding from INFN, FBK and the European Unions Horizon Europe research and innovation programme under grant agreement No 101057511. The authors received research support from institutes as specified in the author list below the title.

## Acknowledgments

The present work is largely the result of the efforts and ingenuity of Andrea Alici, who unfortunately passed away just a few days before its publication. His memory will live on among his colleagues.

## References

- [1] F. Carnesecchi et al., *Direct detection of charged particles with SiPMs*, *Journal of Instrumentation* **17** (2022) .
- [2] F. Carnesecchi et al., *Understanding the direct detection of charged particles with SiPMs*, *Eur. Phys. J. Plus* **138** (2023) 337.
- [3] F. Carnesecchi et al., *Measurements of the Cherenkov effect in direct detection of charged particles with SiPMs*, *Eur. Phys. J. Plus* **138** (2023) 788.
- [4] F. Carnesecchi et al., *Measurements of efficiency, timing and response to irradiation for direct detection of charged particles with SiPMs*, *Submitted to Eur. Phys. J. Plus* (2025) .
- [5] A. Mazzi et al., *SiPM development at FBK for the barrel timing layer of CMS*, 2020.
- [6] A. Altamura et al., *Characterization of Silicon Photomultipliers after proton irradiation up to  $10^{14} \text{ neq/cm}^2$* , *Nuclear Instruments and Methods in Physics Research Section A* **1040** (October 2022) .
- [7] A. Altamura et al., *Radiation damage on SiPMs for space applications*, *NIMA* **1045** (2023) 167488.
- [8] A. Gola et al., *NUV-Sensitive Silicon Photomultiplier Technologies Developed at Fondazione Bruno Kessler*, *Sensors* **19** (2019) .
- [9] S. Gundacker et al., *On timing-optimized SiPMs for Cherenkov detection to boost low cost time-of-flight PET*, *Physics in Medicine & Biology* **68** (2023) .

- [10] M. Van Dijk et al., *Particle production and identification for the T10 secondary beamline of the CERN East Area*, 2025.
- [11] F. Carnesecchi et al., *Beam test results of 25  $\mu\text{m}$  and 35  $\mu\text{m}$  thick FBK ultra fast silicon detectors*, *The European Physical Journal Plus* **138** (2023) .
- [12] S. Umarov, C. Tsallis and S. Steinberg, *On a  $q$ -Central Limit Theorem Consistent with Nonextensive Statistical Mechanics*, *Milan J. Math* **76** (12,2008) 307.
- [13] I.M. Frank and I.E. Tamm, *Coherent radiation of fast electrons in a medium.*, *Dokl. Akad. Nauk SSSR* **14** (1937) 109.
- [14] A. Mazzi et al., *NUV-HD SiPMs with metal-filled trenches*, *Journal of Instrumentation*. **18** (2023) .